Performance Verification of a Variable Bit-Rate Limiter for On–Off Keying (OOK) Optical Systems

Yong-Gang Wen, Lian-Kuan Chen, Keang-Po Ho, Frank Tong, and Wai-Shan Chan

***Abstract*—A close-form analytical expression is obtained for the performance study of a bit-rate limiter (BRL). Both bit-error rate (BER) and power penalty are derived for different BRL modulation signals and modulation formats using a random signal model. We also present ways to improve the BRL performance and to eliminate the BRL-induced crosstalk, by using an optimal BRL modulation index and a specific BRL modulation signal, respectively. The analytical expression is found to match well with the experimental measurements.**

***Index Terms*—Bit-rate limiter (BRL), crosstalk suppression, on–off keying (OOK) optical fiber link, optical transmission system, Mach–Zehnder (MZ) modulator, power penalty.**

I. INTRODUCTION

With the inherent enormous bandwidth in the fiber, communication based on optical fibers is an excellent candidate to accommodate the exponential growth in data traffic engendered by the Internet. With the recent advances in wavelength-division-multiplexing (WDM) technologies, in which the bandwidth in the optical fiber can be partitioned into many channels, the economic values generated from an optical link and network are tremendous. To the owners of the fiber links and the future all-optical transparent networks, it becomes essential to devise a means to ensure the certified users will not transmit digital data at a rate higher than that is allowed by their subscription fees. Such means can be realized as a device, i.e., bit-rate limiter (BRL), and can impose a limit on the transmission data rates. To inflict less restriction on the customer, the BRL is preferably wavelength independent, and must neither interfere nor tap the transmitting data to ensure data privacy.

Conceptually, BRL can be implemented by two different approaches. The first is to use an optical narrow band-pass filter (BPF) that cuts off the out-of-band data spectrum. However, in general, optical BPF is wavelength-dependent and has a fixed or tunable central wavelength. Furthermore, the passband bandwidth cannot be varied in accordance to the users' request of different data rates. The second approach is to generate an interference signal to jam out-of-band data spectrum. In this approach, two types of all-fiber BRL were proposed previously [1], [2]. One design uses a fiber recirculating delay line with a loop delay of τ to limit the nonreturn-to-zero (NRZ) transmission rate to slightly below $1/\tau$ b/s. The insertion loss of this type of device can be less than 1 dB and can be installed at any point along the fiber link. The other design, based on a special dual-mode fiber, makes use of the two equally propagating modes but with noticeably different group velocities. In either design, the incident optical field amplitudes are added to that in the delay replicas, generating dispersion-like interference that limits the transmission data rate. However, the optical wave also beats with its replicas and produces interferometric noise at the receiver. As such, laser phase noise is converted to relative intensity noise (RIN), resulting in error-rate floor that can be very substantial, even when system is operating at bit rates well below the device cutoff rate of $1/\tau$ [3]. Moreover, neither scheme offers a variable bit-rate capability, which restricts their use in practical systems that may need to change its limiting data rates after installation. In this paper, we provide an analytic and experimental performance verification of a previously proposed BRL [10]. The principle of operation is based on self-generated aliasing interference from modulation. Using only an external modulator, the BRL is nonintrusive in nature and is wavelength insensitive. Such device can impose efficient limits on user's data rate, and eliminate the bit-error rate (BER) floor exhibited in the previous designs. The BRL can also support variable limiting data rates.

This paper is organized as follows. In Section II, a brief description of the operating principle of the BRL is presented. The detailed analysis of the BRL, including BER performance and power penalty, is given in Section III. The analytical result of the power penalty provides insight for system bandwidth management. We further define two performance metrics to characterize the BRL. In Section IV, the analytical results are compared with experimental results and found to be consistent. Section V discusses some factors that affect the performance of our scheme. Further enhancements of the BRL scheme are presented and the power penalty curves of these enhanced schemes are shown. Section VI concludes this paper.

II. PRINCIPLE OF THE BIT-RATE LIMITER

The proposed BRL scheme is based on the aliasing effect of modulation and requires only an optical modulator inserted anywhere in the optical fiber between the two end terminals of an OOK modulated system. Fig. 1 shows the schematic diagram of our modulating scheme.

Passing through the modulator, an NRZ optical signal at data-rate f_d is modulated by a sinusoidal signal, called the BRL

Manuscript received November 30, 1999. This work was supported by the Hong Kong Government RGC Earmarked Grant CUHK4153/98E.

Y.-G. Wen, L.-K. Chen, K.-P. Ho, and F. Tong are with the Lightwave Communications Laboratory, Department of Information Engineering, The Chinese University of Hong Kong, Shatin, N.T., Hong Kong, China (e-mail: ygwen9@ie.cuhk.edu.hk).

W.-S. Chan is with AT&T Global Network Services, Chai Wan, Hong Kong, China.

Publisher Item Identifier S 0733-8724(00)05081-7.

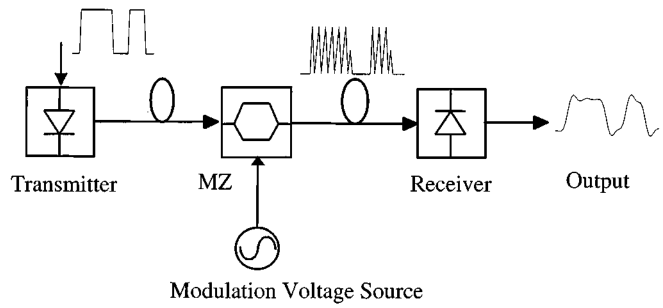

Fig. 1. Modulation BRL scheme (MZ = Mach-Zehnder modulator).

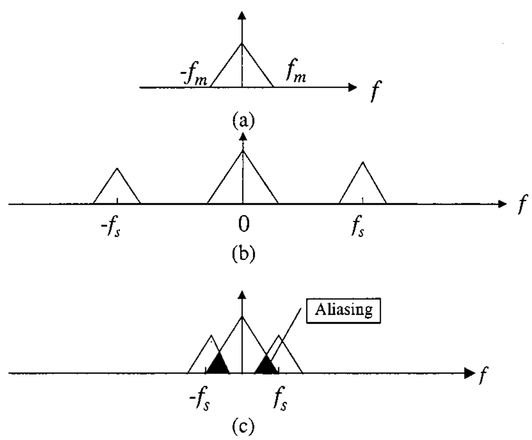

Fig. 2. The principle of the BRL scheme. (a) The PSD of the original signal. (b) The PSD of the BRL modulated signal, $f_s > 2f_m$. (c) The PSD of the BRL modulated signal, $f_s > 2f_m$.

modulation signal, with a frequency f_s. After the modulator, the replicas of the signal power spectrum are generated at high harmonics frequencies, nf_s, $n = 2, 3, \ldots$. When f_s is much faster than f_d, at least two times of f_d [4], the replicas at higher frequency will not overlap with the baseband waveform and can be eliminated by a low-pass filter (LPF) in the receiver, as shown in Fig. 2(b). Otherwise, the power of lower order harmonics replica will overlap with the baseband signal spectrum and cannot be eliminated by the LPF in the receiver, as shown in Fig. 2(c). This will result in an increase in BER, even a BER floor. When users try to deprive more bandwidth of the leased fiber by increasing their data rate f_d, more interference will generate, resulting in very high power penalty. In order to get the same BER performance, the output power of the transmitter must be increased substantially. Thus the proposed device can prevent the unauthorized usage of extra bandwidth in a leased fiber. On the other hand, when a user wishes to increase his leased data rate, the network manager can cater the request by simply increasing f_s of the user's BRL device. Thus the BRL facilitates network management for dynamic bandwidth allocation. In the following section, we derive an analytical expression of the power penalty imposed by the BRL to show its effectiveness in bit-rate limiting.

III. Analysis of the Bit-Rate Limiter

A. BER Analysis

After the photodetector in the receiver, the received current is

$$r(t) = RKs_0(t)g(t) + n_{\mathrm{th}}(t) + n_{\mathrm{sh}}(t) + n_{\mathrm{RIN}}(t) \quad (1)$$

where R is the responsivity of the photodetector, K is the attenuation factor, $n_{\mathrm{th}}(t)$ is the thermal noise, $n_{\mathrm{sh}}(t)$ is the shot noise, $n_{\mathrm{RIN}}(t)$ is the relative intensity noise (RIN), $s_0(t)$ is the original signal, and $g(t)$ is the modulation function of the optical modulator.

According to the bias voltage of the MZ modulator, two types of $g(t)$ are considered, namely,

$$g_1(t) = 1 + \cos\left(\frac{V}{V_\pi} \cdot \pi\right) \quad (2)$$

$$g_2(t) = 1 + \sin\left(\frac{V}{V_\pi} \cdot \pi\right) \quad (3)$$

where V is the modulation signal, V_π is the difference of the biased voltages to switch the output power from a maximum point to the adjacent minimum point.

Assume the BRL modulation frequency is ω_s, and the BRL modulation signal is given by $V = V_\pi \cos(\omega_s t + \Phi)/2$, where Φ is the random initial phase, with uniform distribution in $[0, 2\pi)$. From Taylor series expansion and the definition of Bessel function, $g_1(t, \Phi)$ can be expressed as

$$\begin{aligned} g_1(t, \Phi) &= 1 + \cos\left[\frac{\pi}{2}\cos(\omega_s t + \Phi)\right] \\ &= (1 + a_0) + \sum_{k=1}^{\infty} a_k \cos(2k\omega_s t + 2k\Phi) \end{aligned} \quad (4)$$

where

$$a_0 = \frac{1}{2\pi}\int_0^{2\pi} \cos\left[\frac{\pi}{2}\cos(\omega_s t)\right] dt = J_0\left(\frac{\pi}{2}\right)$$

and

$$\begin{aligned} a_k &= \frac{1}{\pi}\int_0^{2\pi} \cos\left[\frac{\pi}{2}\cos(\omega_s t)\right] \cos(2k\omega_s t)\, dt \\ &= 2(-1)^k J_{2k}\left(\frac{\pi}{2}\right) \end{aligned}$$

are the series expansion coefficients [11]. In this paper, we consider only the first N leading terms a_k, $k = 1$ to N, and neglect the higher order terms.

Before LPF filtering, the autocorrelation function of the received signal is

$$\begin{aligned} R_r(\tau) &= R^2K^2R_0(\tau)E[g(t, \Phi)g(t - \tau, \Phi)] \\ &\quad + R_{\mathrm{th}}(\tau) + R_{\mathrm{sh}}(\tau) + R_{\mathrm{RIN}}(\tau) \end{aligned} \quad (5)$$

where $E[\bullet]$ denotes the expectation value, $R_{\mathrm{th}}(\tau)$, $R_{\mathrm{sh}}(\tau)$ and $R_{\mathrm{RIN}}(\tau)$ are the auto-correlation function of $n_{\mathrm{th}}(t)$, $n_{\mathrm{sh}}(t)$ and $n_{\mathrm{RIN}}(t)$, respectively. With (4), and considering the case $g(t) = g_1(t)$, we obtain

$$\begin{aligned} &E[g(t, \Phi)g(t - \tau, \Phi)] \\ &\quad = (1 + a_0)^2 + \frac{1}{2}\sum_{k=1}^{N} a_k^2 \cos(2k\omega_s \tau). \end{aligned} \quad (6)$$

After substituting (6) into (5), $R_r(\tau)$ is given by

$$\begin{aligned} R_r(\tau) = &R^2K^2R_0(\tau)(1+a_0)^2 \\ &+ \frac{1}{2}R^2K^2R_0(\tau)\sum_{k=1}^{N} a_k^2\cos(2k\omega_s\tau) \\ &+ R_{\rm th}(\tau) + R_{\rm sh}(t) + R_{\rm RIN}(\tau). \end{aligned} \tag{7}$$

According to Wiener-Khintchine theorem [5], the power spectral density (PSD) of the received signal $r(t)$ is

$$\begin{aligned} S_r(\omega) =& R^2K^2S_0(\omega)(1+a_0)^2 \\ &+ \sum_{k=1}^{N}\frac{1}{4}R^2K^2a_k^2[S_0(\omega-2k\omega_s)+S_0(\omega+2k\omega_s)] \\ &+ S_{\rm th}(\omega)+S_{\rm sh}(\omega)+S_{\rm RIN}(\omega) \\ =& S_1(\omega)+S_a(\omega)+S_s(\omega) \end{aligned} \tag{8}$$

where

$$\begin{aligned} S_1(\omega) &= R^2K^2S_0(\omega)(1+a_0)^2 \\ S_a(\omega) &= \frac{1}{4}\sum_{k=1}^{N} R^2K^2a_k^2[S_0(\omega-2k\omega_s)+S_0(\omega+2k\omega_s)] \\ S_s(\omega) &= S_{\rm th}(\omega)+S_{\rm sh}(\omega)+S_{\rm RIN}(\omega) \end{aligned}$$

Assume the transfer function of LPF is $H(\omega)$ and its 3-dB bandwidth is $\omega_{3\,\rm dB} = \Delta\omega$. After filtering

$$I = \int_{-\Delta\omega}^{\Delta\omega} R^2K^2(1+a_0)^2S_0(\omega)|H(\omega)|^2\,d\omega \tag{9}$$

$$N = \int_{-\Delta\omega}^{\Delta\omega}[S_a(\omega)+S_s(\omega)]\cdot|H(\omega)|^2\,d\omega \tag{10}$$

where I is the desired signal power and N is the total noise power. The noise power N consists of two components, namely, the system noise power N_s

$$N_s = \int_{-\Delta\omega}^{\Delta\omega}[S_{\rm th}(\omega)+S_{\rm sh}(\omega)+S_{\rm RIN}(\omega)]\cdot|H(\omega)|^2\,d\omega$$

and the BRL-induced interference power N_a

$$N_a(\omega_s) = \int_{-\Delta\omega}^{\Delta\omega} S_a(\omega)\cdot|H(\omega)|^2\,d\omega \tag{11}$$

Notice that N_a is the intentionally generated interference to limit the system data rate and it is a function of the BRL modulation frequency ω_s $(=2\pi f_s)$. Subsequently, the signal to noise ratio (SNR) can be expressed as

$$\mathrm{SNR} = \frac{I}{N_s+N_a(\omega_s)}, \tag{12}$$

For OOK modulation data with direct detection, the BER is given by [6]

$$\mathrm{BER} = \frac{1}{2}\,\mathrm{erfc}\left(\frac{Q}{\sqrt{2}}\right) = \frac{1}{2}\,\mathrm{erfc}\left(\sqrt{\frac{\mathrm{SNR}}{8}}\right). \tag{13}$$

Without loss of generality, the transmitted data is assumed an equal-probable binary stream. Its auto-correlation function is [7]

$$R_0(\tau) = \begin{cases} A^2\left(1-\frac{|\tau|}{T}\right), & |\tau|\le T \\ 0, & \text{otherwise} \end{cases} \tag{14}$$

where A is the amplitude of the bit stream and T is the bit duration. The power spectral density of the binary stream is

$$S_0(\omega) = \int_{-\infty}^{\infty} R_0(\tau)e^{-j\omega\tau}\,d\tau = A^2T\left|\frac{\sin\left(\frac{\omega T}{2}\right)}{\frac{\omega T}{2}}\right|^2. \tag{15}$$

From (11), (8), and (15), we can calculate the BRL-induced interference power $N_a(\omega_s)$.

The system noise power N_s

$$N_s = \int_{-\Delta\omega}^{\Delta\omega}[S_{\rm th}(\omega)+S_{\rm sh}(\omega)+S_{\rm RIN}(\omega)]\cdot|H(\omega)|^2\,d\omega$$

is generated from three components: $S_{\rm th}(\omega)$ thermal noise, $S_{\rm sh}(\omega)$ shot noise, and $S_{\rm RIN}(\omega)$ relative intensity noise. The respective noise spectral and corresponding noise powers are derived in the Appendix.

B. Power Penalty

An important factor of the proposed device is its effectiveness in bit-rate limiting. This can be deduced from the power penalty when the user tries to increase its transmission data-rate without authorization.

For the back-to-back system without BRL modulation, the SNR is given by

$$\mathrm{SNR}_{B\text{-}B} = \frac{\int_{-\Delta\omega}^{\Delta\omega} R^2K^2S_0^{\rm B\text{-}B}(\omega)|H(\omega)|^2\,d\omega}{\int_{-\Delta\omega}^{\Delta\omega} S_s^{\rm B\text{-}B}(\omega)\cdot|H(\omega)|^2\,d\omega} \tag{16}$$

where $S_s^{\rm B\text{-}B}(\omega) = S_{\rm th}(\omega)+S_{\rm sh}^{\rm B\text{-}B}(\omega)+S_{\rm RIN}^{\rm B\text{-}B}(\omega)$ and the superscript and subscript, B-B, denote the back to back system. While for the system with BRL device, the SNR is

$$\mathrm{SNR}_{\rm BRL} = \frac{\int_{-\Delta\omega}^{\Delta\omega} R^2K^2(1+a_0)^2S_0^{\rm BRL}(\omega)|H(\omega)|^2\,d\omega}{\int_{-\Delta\omega}^{\Delta\omega}[S_a^{\rm BRL}(\omega)+S_s^{\rm BRL}(\omega)]\cdot|H(\omega)|^2\,d\omega} \tag{17}$$

where

$$\begin{aligned} S_a^{\rm BRL}(\omega) =& \sum_{k=1}^{N}\frac{1}{4}R^2K^2a_k^2 \\ &\cdot\left[S_0^{\rm BRL}(\omega-2k\omega_s)+S_0^{\rm BRL}(\omega+2k\omega_s)\right] \\ S_s^{\rm BRL}(\omega) =& S_{\rm th}(\omega)+S_{\rm sh}^{\rm BRL}(\omega)+S_{\rm RIN}^{\rm BRL}(\omega). \end{aligned}$$

By equating $\mathrm{SNR}_{\rm B\text{-}B} = \mathrm{SNR}_{\rm BRL}$, we can derive the power penalty

$$\begin{aligned} p &= \frac{S_0^{\rm BRL}(\omega)}{S_0^{\rm B\text{-}B}(\omega)} \\ &= \frac{1}{(1+a_0)^2 - \frac{N_a(\omega_s)-a_0(a_0+2)\left(N_{\rm sh}^{\rm B\text{-}B}+N_{\rm RIN}^{\rm B\text{-}B}\right)}{N_{\rm th}}}. \end{aligned} \tag{18}$$

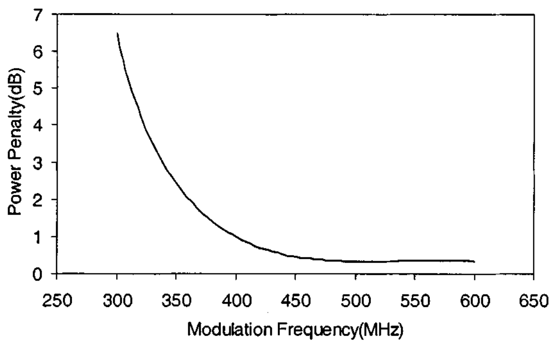

Fig. 3. Power Penalty with fixed Data Rate, Data rate $f_d = 600$ Mb/s, and BRL modulation function $g_1(t)$.

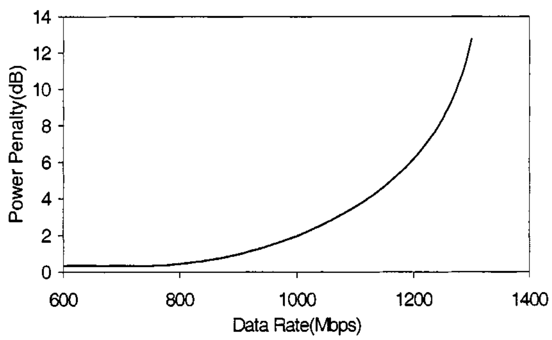

Fig. 4. Power Penalty with fixed modulation frequency $f_s = 600$ MHz and BRL modulation function $g_1(t)$.

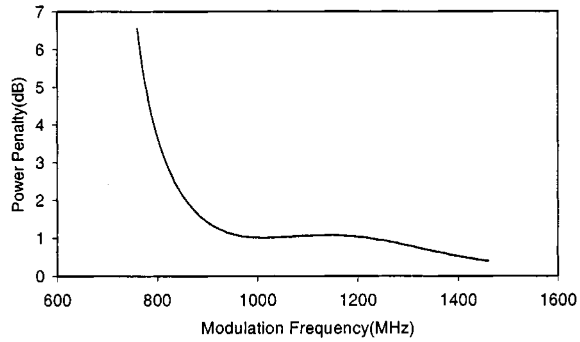

Fig. 5. Power penalty with fixed data rate $f_d = 600$ Mb/s and BRL modulation function $g_2(t)$.

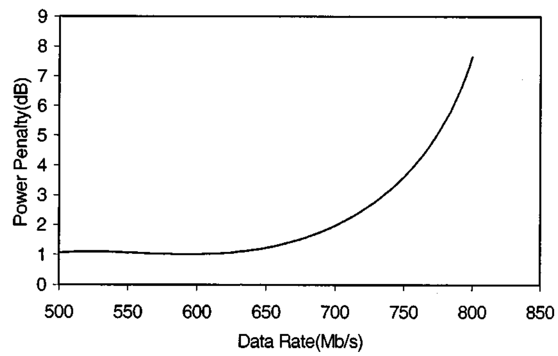

Fig. 6. Power penalty with fixed modulation frequency $f_s = 1000$ MHz and BRL modulation function $g_2(t)$.

In practical digital systems, thermal noise usually is dominant over shot noise and relative intensity noise. Thus we can neglect their effects and obtain a simple expression of power penalty as

$$\delta_d = 10\log(p) = -10\log\left[(1+a_0)^2 - \frac{N_a(\omega_s)}{N_{\text{th}}}\right]. \quad (19)$$

Fig. 3 shows the power penalty calculated from (19) with data rate $f_d = 600$ Mb/s and modulation frequency f_s ranging from 300 MHz to 600 MHz. The system parameters are the following: the temperature $T = 298$ K, the amplifier noise figure $F_n = 2.5$, the load resistor $R_L = 300\ \Omega$. In Fig. 3, $g_1(t) = 1 + \cos(\pi \cdot V/V_\pi)$, and $V = V_\pi \cos(\omega_s t + \Phi)/2$. From the figure, when f_s is about 400 MHz, the power penalty is about 1 dB. With the reduction of f_s, the power penalty rises sharply. The modulation frequency $f_s = 400$ MHz will limits the user's data rate below 600 Mb/s, assuming the acceptable power penalty is 1 dB.

In order to show the bit-rate limiting capability for the data rate using our BRL scheme, Fig. 4 depicts another power penalty curve with variable data rate ranging from 600 Mb/s to 1400 Mb/s and a fixed modulation frequency $f_s = 600$ MHz. Other conditions are the same as those of Fig. 3. From Fig. 4, when f_d is about 900 Mb/s, the power penalty is about 1 dB. With an increasing data rate f_d, the power penalty increases steeply, demonstrating the effectiveness of the proposed BRL device.

C. BRL Efficiency

Analogous to the parameters of a low-pass filter (LPF), two parameters are defined to characterize the performance of the BRL scheme. One is the cutoff data rate F_d that is defined by the data rate with power penalty 1 dB. The other is the normalized slope of 3 dB-to-1 dB point

$$\Delta = \frac{F_d}{f_d\,(3\text{ dB}) - f_d\,(1\text{ dB})}. \quad (20)$$

The expression f_d (x dB) denotes the data rate at power penalty of x dB. Notice that $F_d = f_d$ (1 dB). From Fig. 4, $F_d = 900$ Mb/s and $\Delta = 3.534$. A larger Δ gives a better BRL performance with steep increase in power penalty when the user data exceeds the cutoff data rate. In next section, we will introduce method to increase Δ.

Moreover, we will consider the BRL performance for the other modulation function $g_2(t)$. The bias voltage of the modulator can be set at the half-maximum point to realize a BRL modulating function $g_2(t) = 1 + \sin(V \cdot \pi/V_\pi)$ with $V = V_\pi \cos(\omega_s t + \Phi)/2$. Two power penalty curves are plotted using (19). Fig. 5 is for a fixed data rate $f_d = 600$ Mb/s and BRL modulation frequency ranging from 600 MHz to 1600 MHz, whereas Fig. 6 is for a fixed modulation frequency $f_s = 1000$ MHz and data rate ranging from 500 Mb/s to 1000 Mb/s. The cutoff data rate $F_d = 650$ Mb/s and the slope $\Delta = 7.194$ can be obtained from Fig. 6. Comparing Fig. 4 with Fig. 6, we can find that the modulator function can affect the cutoff frequency F_d and the slope Δ. With the same data rate, the required BRL modulation frequency is different. For example, for a data bit rate $f_d = 600$ Mb/s, a BRL modulation signal with frequency $f_s = 400$ MHz can impose 1-dB power penalty using $g_1(t) = 1 + \cos(\pi \cdot V/V_\pi)$, whereas a BRL modulation frequency $f_s = 900$ MHz is required using $g_2(t) = 1 + \sin(V \cdot \pi/V_\pi)$. This

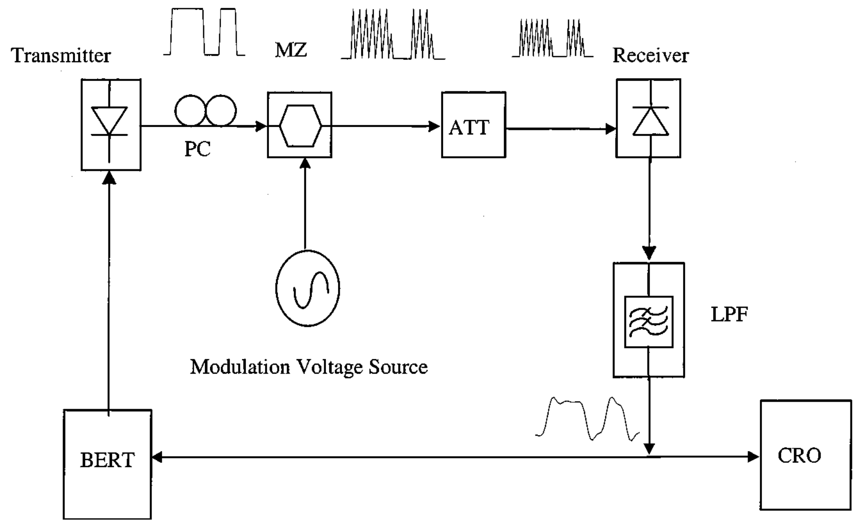

Fig. 7. Experimental setup (PC = polarization controller; MZ = Mach–Zehnder Interferometric switch; ATT = optical attenuator; LPF = low-pass filter; CRO = oscilloscope; BERT = bit-error rate tester and data pattern generator).

phenomenon can be understood as $g_1(t)$ poses a frequency-doubling property [8], [9]. Thus biasing at the maximum point is better than at half-maximum point. On the other hand, the slope Δ of the former modulation is smaller than that of the latter. Therefore, there is a tradeoff between the larger slope Δ and lower BRL modulation frequency.

IV. Comparison of the Analytical and Experimental Results

We verify the effectiveness of our scheme and validity of our analysis with an experimental system as showed in Fig. 7 [10]. A distributed feedback (DFB) laser with a center wavelength 1555 nm is used as the transmitter. An optical MZ modulator is used to impose the BRL modulation. The modulator has an insertion loss of about 3 dB and an extinction ratio of about 26 dB. A high-speed RF signal generator is used to generate the required BRL modulation signal to drive the modulator. The receiver is a p-i-n receiver with a bandwidth of 1.6 GHz. Because of the large receiver bandwidth, an RF-LPF is attached to the receiver output to further narrow down the receiver bandwidth.

The modulator is biased at half-maximum point, and the peak amplitude of the sinusoidal modulation signal is set to $V_\pi/2$, that is

$$g_1(t,\Phi) = 1 + \sin\left(\frac{\pi}{2}\cos(\omega_s t + \Phi)\right).$$

With a fixed signal frequency at $f_s = 800$ MHz, we vary the data rate and measure the power penalty. Fig. 8 shows both the experimental results and the analytical results derived under the same conditions. From Fig. 8, there is only a small deviation between the experimental and analytical results. Fig. 8 successfully demonstrates that the proposed BRL scheme can limit the user data rate. Another experiment was conducted using fixed data rate $f_d = 600$ Mb/s with varying modulation frequency. Fig. 9 also shows that the analytical results again agree well with the experimental results.

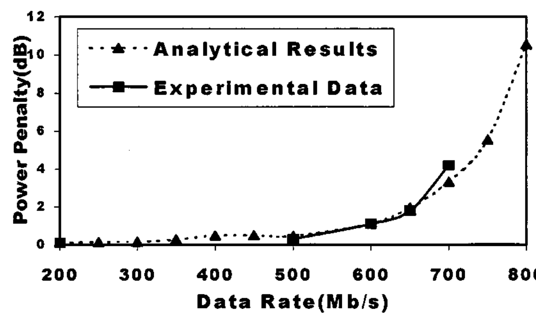

Fig. 8. Comparison between the analytical and experimental results. Analytical results are derived from (19). The experiment is for $f_s = 800$ MHz, data rate f_d varying from 200 Mb/s to 800 Mb/s ($2^{10} - 1$ PRBS,NRZ), and the 3-dB bandwidth of the RF filter is $0.75 * f_d$ MHz.

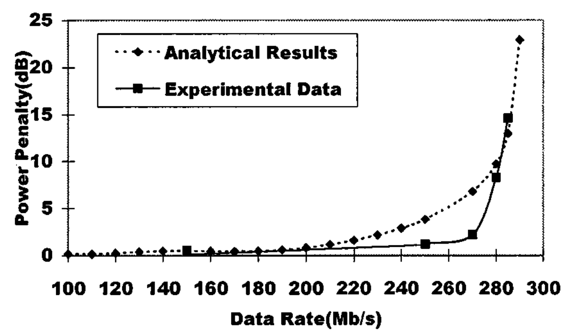

Fig. 9. Comparison of power penalty between the analytical and experimental results. Analytical results are derived from (19). The experimental is for $f_s = 275$ MHz and f_d varying from 100 Mb/s to 300 Mb/s ($2^{10} - 1$ PRBS,NRZ). The RF filter bandwidth is 205 MHz.

V. Optimization of the Bit-Rate-Limiter

The performance of the BRL can be improved by choosing some optimal parameters for the modulation index and the BRL modulation function. The objectives are 1) to induce minimum power penalty when the data rate is below the specified data rate, 2) to give very high power penalty when data rate exceeds

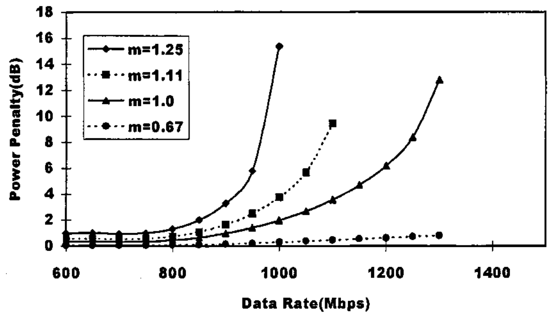

Fig. 10. Power penalty for variable m. BRL modulation frequency $f_s = 600$ MHz and BRL modulation function $g_1(t)$.

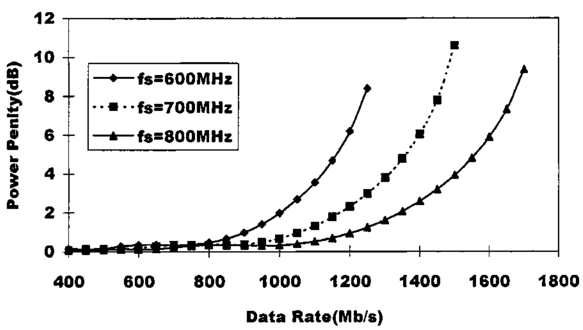

Fig. 11. Varification of independence between the passband power penalty and the BRL modulation frequency f_s for a fixed modulation index $m = 1.0$. BRL modulation frequency f_s is 600 MHz, and BRL modulation function is $g_1(t)$.

the leased data rate, and 3) to give no BRL-induced crosstalk to adjacent channel. We have shown that the normalized slope Δ is one of the appropriate criteria to assess the BRL performance of the proposal scheme. A larger Δ gives a better bit-rate limiting effect. Resulting from the BRL-induced interference power, the slope Δ is a function of Taylor expansion's coefficients of the modulation function.

A. Optimization of Normalized Slope and Passband Power Penalty

Based on (4), different BRL modulation amplitudes are investigated to realize a better Δ. In Fig. 10, the power penalty curves with different modulation amplitudes are presented. In the analysis, the BRL modulation index parameter m is used, and is related to the BRL modulation signal amplitudes by $m = 2V_0/V_\pi$ where V_0 is the signal amplitude. From Fig. 10, with the increase of modulation index m, the slope Δ increases gradually from 5.29 $(m = 1.0)$ to 7.13 $(m = 1.25)$, resulting in a better BRL performance. However, when m is increased, it also induces a higher power penalty even for data rate below the leased bandwidth, i.e., higher passband power penalty. A proper m should be chosen to balance this performance tradeoff.

Fig. 11 plots different power penalty curves for different modulation frequency f_s and a fixed $m = 1.0$. Fig. 11 shows that the passband power penalty is almost independent of f_s for a fixed $m = 1.0$. Assume that the acceptable maximum power penalty induced by this device is 1 dB. An optimal index m to give the best BRL performance can then be found by choosing the m that induces a 1-dB power penalty at the leased data rate. Fig.

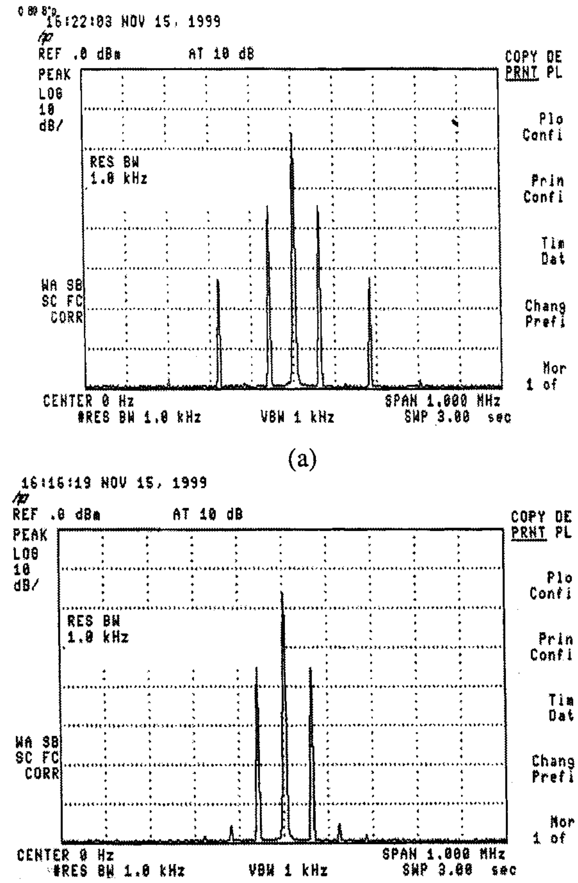

(a)

(b)

Fig. 12. Spectral density of BRL modulator signal with two different BRL modulation signals using $g_2(t)$. (a) Sinusoid waveform and (b) triangular waveform.

10 provides an optimal index $m = 1.25$ for the BRL modulation function $g_1(t) = 1 + \cos(\pi \cdot V/V_\pi)$ with a BRL modulation signal $V = V_\pi \cos(\omega_s t + \Phi)/2$. Note that this optimal m depends on the modulation function.

B. Suppression of BRL-Induced Crosstalk

Based on (8), the modulated signal would spread its spectral content to higher frequencies. The replicas of signal power spectral waveform are generated, with descending power, at higher frequencies with a frequency spacing of $2f_s$. In future dense WDM (DWDM) systems, the wavelength channel spacing can be very compact, possibly only several times of data rate, e.g., 3–6 times, depending on the discriminating ability of the wavelength multiplexers and demultiplexers. Thus, upon being modulated by BRL, the higher order harmonics of signal spectral may drop into adjacent channels. This will result in BRL-induced crosstalk that can degrade system performance. The BRL scheme is suitable for WDM system in which different users share a common fiber, thus it is desirable to reduce the crosstalk of the proposed BRL scheme. Here, we propose to use a particular BRL modulation signal that can totally eliminate the crosstalk.

Considering the Taylor series expansion of the modulation function, it is possible to eliminate the higher order harmonics if a proper BRL modulation signal format is used to drive the modulator. For the BRL modulation function $g_1(t) = 1+\cos(\pi \cdot V/V_\pi)$, the function will become $g_1(t) = 1 + \cos(\omega_s \cdot t)$ if the BRL modulation signal is chosen to be a triangular waveform

$$V = \sum_{l=-\infty}^{\infty} V_0(t - 2lT) \tag{21}$$

$$V_0(t) = \begin{cases} V_\pi \left(2 - \dfrac{\omega_s}{\pi} \cdot |t|\right) & -T < t < T \\ 0, & \text{otherwise} \end{cases} \tag{22}$$

with $T = 2\pi/\omega_s$. In this case, only the first order harmonics exits and the optical signal power that leaks into adjacent channels is minimized. Thus BRL-induced crosstalk is negligible, further improving the proposed BRL scheme for DWDM systems. Using the new BRL modulation signal, we can obtain the same bit-rate limiting performance without adjacent channel interference. In Fig. 12, the spectral of two modulation functions are compared. From Fig. 12(a), we can see that the odd order harmonics exists when the BRL modulation signal is a sinusoid waveform. On the other hand, when the periodic triangular waveform is used instead, almost only the first order harmonics exists as shown in Fig. 12(b). The dramatic reduction in the higher order harmonics implies that closer channel spacing is allowed.

VI. Conclusion

In this paper, an analytical model is constructed for a bit-rate limiting device proposed previously. Closed-form analytical formulas are derived for both BER and power penalty. The analytical results are consistent with the experimental measurements. Two performance metrics, the cutoff data rate F_d and the normalized 3 dB-to-1 dB slope Δ, are used to characterize the performance of the different BRL schemes.

With these two parameters, we analyze various schemes to improve the BRL performance, and to reduce the BRL-induced crosstalk in DWDM systems. Good BRL performance can be achieved with carefully chosen signal amplitude, which is required to balance between the tradeoff of passband power penalty and normalized slope. By 1-dB pass-band power penalty rule, an optimal index $m = 1.25$ is found for the BRL modulation function $g_1(t) = 1 + \cos(\pi \cdot V/V_\pi)$.

A periodic triangular waveform is proposed for the BRL modulation signal. Such waveform can further minimize BRL induced crosstalk, and is very desirable for DWDM systems.

Appendix
Respective Power of Three Kinds of System Noises

Mathematically, thermal noise can be modeled as a stationary Gaussian random process with a constant spectral density for frequency up to ∼1 THz, and is given by

$$S_{\text{th}}(\omega) = 2k_BT/R_L \tag{23}$$

where k_B is the Boltzmann constant, T is the absolute temperature, and R_L is the load resistor. Formula (19) includes only the thermal noise generated by the load resistor. However, an actual receiver consists of many other electrical components, resulting in additional noises. Taking into the consideration of preamplifier, we can rewrite the formula (23) into

$$S_{\text{th}}(\omega) = \frac{2k_BT}{R_L} \cdot F_n, \tag{24}$$

where F_n is the amplifier noise figure. After filtering, the thermal noise power is given by

$$\begin{aligned} N_{\text{th}} &= \int_{-\Delta\omega}^{\Delta\omega} S_{\text{th}}(\omega) \cdot |H(\omega)|^2 \, d\omega \\ &= \frac{2k_BT}{R_L} \cdot F_n \cdot \int_{-\Delta\omega}^{\Delta\omega} |H(\omega)|^2 \, d\omega. \end{aligned} \tag{25}$$

Shot noise originates from the random generation of photoelectrons that in turn generates the electric current. Basically, shot noise is a stationary random process with Poisson statistics, which can be approximated by the Gaussian statistics in practice. The spectral density of shot noise is constant, and is given by

$$S_{\text{sh}}(\omega) = eI_p \tag{26}$$

where e is the electron charge and I_p is the average received photo current. The photocurrent I_p is given by

$$I_p = R \cdot P_{\text{in}}. \tag{27}$$

where R is the responsivity and P_{in} is the incident optical power

$$P_{\text{in}} = \frac{1}{2\pi} \int_{-\infty}^{\infty} S_0(\omega) \, d\omega. \tag{28}$$

After filtering, the shot noise power is

$$\begin{aligned} N_{\text{sh}} &= \int_{-\Delta\omega}^{\Delta\omega} S_{\text{sh}}(\omega) \cdot |H(\omega)|^2 \, d\omega \\ &= \int_{-\Delta\omega}^{\Delta\omega} |H(\omega)|^2 \, d\omega \cdot eR \cdot \int_{-\infty}^{\infty} S_0(\omega) \, d\omega. \end{aligned} \tag{29}$$

After the low-pass filter, the relative intensity noise (RIN) power is

$$N_{\text{RIN}} = \int_{-\Delta\omega}^{\Delta\omega} |H(\omega)|^2 \, d\omega \cdot R \cdot r_1 \cdot \int_{-\infty}^{\infty} S_0(\omega) \, d\omega. \tag{30}$$

where r_I is a measure of the noise level of the incident optical power [6].

References

[1] V. A. Bhagavatula and D. Charlton, "Bit-rate limiting as an alternative to facility bypass," in *Proc. IEEE ICOC'87*, Seattle, WA, 1987, pp. 198–201.

[2] M. Tur, E. L. Goldstein, C. A. Brackett, R. C. Mendendez, and G. Coquin, "An optical all-fiber bit-rate limiter," in *Proc. 13th ECOC*, Helsinki, Finland, 1987, pp. 385–388.

[3] M. Tur, E. L. Goldstein, and C. A. Brackett, "Effect of laser phase noise on a class of bit-rate limiter," *Electron. Lett.*, vol. 24, no. 2, pp. 126–128, Jan. 21, 1988.

[4] J. G. Proakis, *Digital Communication*. New York: McGraw-Hill, 1995, pp. 94–106.

[5] A. D. Whalen, *Detection of Signals in Noise*. New York: Academic, 1971.

[6] G. P. Agrawal, *Fiber-Optic Communication Systems*. New York: Wiley, 1993, pp. 155–182.

[7] S. G. Wlison, *Digital Modulation and Coding*. Englewood Cliffs, NJ: Prentice Hall, 1996, pp. 60–65.
[8] C. D. Watson, D. A. Humphreys, and M. G. F. Wilson, "Calibration of optical modulators by optical down-conversion," *IEEE Photon. Technol. Lett.*, vol. 5, pp. 1005–1007, Sept. 1993.
[9] K.-P. Ho, S.-K. Liaw, and C. Lin, "Efficient photonic mixer with frequency doubling," *IEEE Photon. Technol. Lett.*, vol. 9, pp. 511–513, Apr. 1997.
[10] W. S. Chan, F. Tong, L. K. Chen, C. K. Chan, and D. Lam, "Variable bit rate limiter for on-off-keying optical links," *Electron. Lett.*, vol. 34, no. 1, pp. 108–110, Jan. 8, 1998.
[11] L.-K. Chen, "Highly linear lightwave video distribution system," Ph.D. dissertation, Columbia University, New York, 1992.

Yong-Gang Wen received the B.S. degree from the Department of Electrical Engineering and Science Information in the University of Science and Technology of China, Hefei, Anhui, China, in 1999.

He is currently a postgraduate student at the Department of Information Engineering of the Chinese University of Hong Kong (CUHK). From 1997 to 1999, he worked as a Research Assistant in the Personal Communication Network and Spread Spectrum Lab of USTC, Hefei, with much attention paid to the G3 mobile communications. Now, he is a Research Assistant in the Lightwave Communications Lab at CUHK. His current research interests include optical code-division multiplexing systems, high-rate optical routing networks.

Lian-Kuan Chen received the B.S. degree from National Taiwan University, Taipei, Taiwan, China, in 1983 and the M.S. and Ph.D. degrees from Columbia University, New York, NY, in 1987 and 1992, respectively.

He had worked at General Instruments for one and a half years before joining The Chinese University of Hong Kong (CUHK), China, in 1992. He has performed research on lightwave video distribution systems with contributions in various distortion reduction schemes for different optical components. His current interests are in broadband local access, ultrahigh-capacity optical networks, and optical network fault and performance management.

Keang-Po Ho received the B.S. degree from National Taiwan University, Taipei, Taiwan, China, in 1991 and the M.S. and Ph.D. degrees from the University of California at Berkeley in 1993 and 1995, respectively, all in electrical engineering.

He performed research in IBM T. J. Watson Research Center, Hawthorne, NY, on all-optical networks in the summer of 1994. He was a Research Scientist with Bellcore, currently Telcordia Technologies, Red Bank, NJ, from 1995 to 1997, conducted research on optical networking, high-speed lightwave systems, and broad-band access. He joined the Department of Information Engineering of the Chinese University of Hong Kong (CUHK), China, in 1997. His current interests include optical communication systems, multimedia communication systems, combined source-channel coding, and communication theory. He has published over 100 journal and conference articles in these fields.

Frank Tong was with IBM Research, first as Research Staff Member and later on as Project Leader, working on multiwavelength optical communication systems. He is currently with The Chinese University of Hong Kong (CUHK), China, in 1996. He has received numerous awards from IBM, including the prestigious IBM Outstanding Innovation Award in 1995. He Frank has authored over 130 papers and 10 patents.

Dr. Tong has been an Associate Editor for IEEE PHOTONICS TECHNOLOGY LETTERS since 1993, and served as program chairman and technical committee member for numerous international conferences.

Wai-Shan Chan, photograph and biography not available at the time of publication.